

Variability of polymorphic families of three types of xylanase inhibitors in the wheat grain proteome

Non Peer-reviewed author version

Courtin, CM; CROES, Kristof; Gebruers, K.; ROBBEN, Johan; NOBEN, Jean-Paul; Samyn, B.; Debyser, G.; Van Beeumen, J. & Delcour, CM (2008) Variability of polymorphic families of three types of xylanase inhibitors in the wheat grain proteome. In: PROTEOMICS, 8(8). p. 1692-1705.

DOI: 10.1002/pmic.200700813

Handle: <http://hdl.handle.net/1942/8274>

1           **Variability of polymorphic families of three types of xylanase**  
2                           **inhibitors in the wheat grain proteome**

3  
4           **Evi Croes<sup>1</sup>, Kurt Gebruers<sup>1</sup>, Johan Robben<sup>2</sup>, Jean-Paul Noben<sup>2</sup>,**  
5           **Bart Samyn<sup>3</sup>, Griet Debyser<sup>3</sup>, Jozef Van Beeumen<sup>3</sup>, Jan A. Delcour<sup>1</sup>,**  
6                           **and Christophe M. Courtin<sup>1</sup>**

7  
8       <sup>1</sup>Laboratory of Food Chemistry and Biochemistry, Department of Microbial and Molecular systems,  
9       Katholieke Universiteit Leuven, Kasteelpark Arenberg 20/2463, B-3001 Leuven, Belgium.

10       <sup>2</sup>Biomedical Research Institute (BIOMED), Hasselt University and School of Life Sciences,  
11       Transnationale Universiteit Limburg, Campus Diepenbeek, B-3590 Diepenbeek, Belgium.

12       <sup>3</sup>Laboratory for Protein Biochemistry and Protein Engineering, Universiteit Gent, K.L. Ledeganckstraat  
13       35, B-9000 Gent, Belgium.

14  
15       **Corresponding author:** Evi Croes, Laboratory of Food Chemistry and Biochemistry,  
16       Katholieke Universiteit Leuven, Kasteelpark Arenberg 20/2463, B-3001 Leuven,  
17       Belgium.

18       Tel.: + 32 16321634. Fax: + 32 16321997.

19       E-mail address: [evi.croes@biw.kuleuven.be](mailto:evi.croes@biw.kuleuven.be).

20  
21       **Abbreviations used:** AC, affinity chromatography; CEC, cation exchange  
22       chromatography; CNBr, cyanogen bromide; GH, glycoside hydrolase;  $\lambda$ PPase,  
23       lambda protein phosphatase; PAA, polyacrylamide; PABs, polyclonal antibodies;  
24       TAXI, *Triticum aestivum* xylanase inhibitor; TFMS, trifluoromethanesulfonic acid;  
25       TLXI, thaumatin-like xylanase inhibitor; XI, xylanase inhibitor; XIP, xylanase  
26       inhibiting protein

27  
28       **Keywords:** polymorphism/wheat/xylanase inhibitors

29 **ABSTRACT**

30 Cereals contain proteinaceous inhibitors of endo- $\beta$ -1,4-xylanases (E.C.3.2.1.8,  
31 xylanases). Since these xylanase inhibitors (XIs) are only active against xylanases of  
32 microbial origin and do not interact with plant endogenous xylanases, they are  
33 believed to act as a defensive barrier against phytopathogenic attack. So far, three  
34 types of XIs have been identified, i.e. *Triticum aestivum* XI (TAXI), xylanase  
35 inhibiting protein (XIP), and thaumatin-like XI (TLXI) proteins. In this study the  
36 variation in XI forms present in wheat grain was elucidated using high-resolution 2-  
37 DE in combination with LC-ESI-MS/MS and biochemical techniques. Reproducible  
38 2-DE fingerprints of TAXI-, XIP-, and TLXI-type XIs, selectively purified from  
39 whole meal of three European wheat cultivars using cation exchange chromatography  
40 (CEC) followed by affinity chromatography (AC), were obtained using a pH-gradient  
41 of 6 to 11 and a molecular mass range of 10 to 60 kDa. Large polymorphic XI  
42 families, not known to date, which exhibit different *pI*- and/or molecular mass values,  
43 were visualised by colloidal CBB staining. Identification of distinct genetic variants  
44 by MS/MS-analysis provides a partial explanation for the observed XI heterogeneity.  
45 Besides genetic diversity, PTMs, such as glycosylation, account for the additional  
46 complexity of the 2-DE patterns.

## 47 **1 INTRODUCTION**

48 Endo- $\beta$ -1,4-xylanases (E.C.3.2.1.8, further referred to as xylanases) are crucial  
49 enzymes in the breakdown of arabinoxylan, the predominant cell wall non-starch  
50 polysaccharide of cereals like wheat [1]. Most of the xylanases are confined to  
51 glycoside hydrolase (GH) families 10 and 11 [2].

52 Little is known about plant endogenous xylanases, which are believed to play a role in  
53 cell wall metabolism, seed germination and pollination [3]. In contrast, a large  
54 number of microbial xylanases has been described. Micro-organisms synthesize these  
55 xylanases, next to other cell wall-degrading enzymes, to provide assimilable nutrients  
56 for development. Moreover, xylanases from phytopathogenic species are important  
57 virulence factors as they facilitate disintegration of plant cell walls at the host  
58 penetration site [4-7]. Several microbial xylanases have been adopted by the paper  
59 and pulp industry to reduce the need for chemical bleaching [8] and by the cereal-  
60 based food and feed industries to improve processing and/or product quality [9-12].

61 One of the strategies of plants to try to impede invasion by microbial pathogens is by  
62 producing antimicrobial agents [13] such as specific enzyme-inhibiting proteins.  
63 These can counteract the action of microbial cell wall-degrading enzymes and hence  
64 limit colonisation, as was demonstrated for polygalacturonase inhibitors present in  
65 several dicotyledonous plants [14].

66 In wheat, three types of xylanase inhibitor proteins (XIs) have been discovered over  
67 the last decade, *i.e.* *Triticum aestivum* XI (TAXI) [15], xylanase inhibitor protein  
68 (XIP) [16], and thaumatin-like XI (TLXI) [17] which, in view of their specificity for  
69 microbial xylanases, and, in the case of TAXI and XIP, their demonstrated  
70 inducibility by pathogens [18, 19], most likely classify as plant defence-related  
71 proteins.

72 TAXI-type XIs are a mixture of high-*pI* inhibitors, TAXI-I to TAXI-IV, with distinct  
73 specificities towards xylanases [18, 20]. They occur simultaneously as a ~40 kDa  
74 single polypeptide and as a processed form existing of two disulfide-linked  
75 polypeptides of ~30 and ~10 kDa [20]. XIP- and TLXI-type XIs are basic, monomeric  
76 proteins with a molecular mass of ~30 and ~18 kDa, respectively [16, 17]. Multiple  
77 putative TAXI- [18, 21, 22] and XIP-type [19, 23] as well as one TLXI-type gene(s)  
78 [17] have been identified in wheat and some have been confirmed. For the three types  
79 of XIs, the existence of various forms as well as differences in their spatio-temporal  
80 location, due to distinct regulatory control mechanisms, have been suggested. Igawa  
81 and co-workers [18, 19] demonstrated that *Taxi-III* and *-IV* transcripts mostly  
82 accumulate in roots and older leaves, in contrast to *Taxi-I*. Furthermore they found  
83 that expression of *Taxi-III* and *Taxi-IV*, in addition to that of *Xip-I*, is pathogen-  
84 inducible. Based on these observations it is speculated that, in analogy with  
85 polygalacturonase inhibitors [24], large families of isoforms have adaptively co-  
86 evolved with antagonistically active microbial xylanases to achieve a superior  
87 counterattack against pathogens. In contrast, *Taxi-I* transcripts are not induced by  
88 infection, suggesting a distinct physiological role *in planta* [18]. Together, the three  
89 types of XIs make up a significant proportion (approx. 2.5%) of the physiologically  
90 active albumin/globulin population, present in wheat grain. Thus, it is logical to  
91 assume that this group of proteins can be of great meaning for the wheat plant. Their  
92 importance in reducing the activity of added microbial xylanases in wheat-based food  
93 processes has already convincingly been demonstrated [25-28] and led to the  
94 development of inhibitor-insensitive xylanases, less prone to year-to-year wheat  
95 inhibitor content variations [29-31].

96 Despite extensive characterization of TAXI-, XIP-, and TLXI-type XIs, there is a lack  
97 of knowledge on their polymorphism in wheat grain. The aim of this study was to  
98 elucidate this unknown heterogeneity using high-resolution 2-DE and subsequent MS  
99 analysis. For the first time a study was undertaken concurrently for the three types of  
100 wheat XIs.

## 101 **2 MATERIALS AND METHODS**

### 102 **2.1 Materials**

103 Wheat cultivars Claire (harvest 2005), Zohra and Koch (harvest 2003) were obtained  
104 from AVEVE (Landen, Belgium) and ground into whole meal using a Cyclotec 1093  
105 sample mill (Tecator, Hogånäs, Sweden). Grindamyl H640 bakery enzyme,  
106 containing a *Bacillus subtilis* GH family 11 xylanase, was purchased from Danisco  
107 (Braband, Denmark). *Penicillium purpurogenum* GH family 10 xylanase was kindly  
108 made available by Prof. Jaime Eyzaguirre (Laboratorio de Bioquímica, Facultad de  
109 Ciencias Biológicas, Pontificia Universidad Católica de Chile, Chile). A GH family  
110 11 xylanase from *Aspergillus niger* and Xylazyme AX tablets, which comprise  
111 azurine cross-linked wheat arabinoxylan, were from Megazyme (Bray, Ireland). All  
112 other reagents, BSA, casein, synthetic peptides and bacteriophage  $\lambda$  protein  
113 phosphatase ( $\lambda$ PPase) were purchased from Sigma-Aldrich (Bornem, Belgium).

114

### 115 **2.2 Extraction of wheat soluble seed proteins**

116 Wheat whole meal was ground in liquid nitrogen using mortar and pestle, and 250 mg  
117 fine powder was suspended in 1.0 ml ice-cold extraction buffer [50 mM Tris-HCl pH  
118 7.8, Complete Protease Inhibitor Cocktail (1 tablet/10 ml buffer, Roche Diagnostics,  
119 Vilvoorde, Belgium)], incubated for 10 min on ice with intermittent mixing and  
120 centrifuged (14000g; 15 min, 4°C). Proteins were precipitated (overnight, -20°C) by  
121 addition of 4 volumes 10% TCA in acetone. Pellets were washed twice with 80%  
122 acetone and air-dried.

123

### 124 **2.3 Purification of xylanase inhibitors from wheat whole meal**

125 Purification of the three types of XIs in wheat whole meal was performed using cation  
126 exchange chromatography (CEC) followed by affinity chromatography (AC) with  
127 immobilised xylanases according to a protocol described by Gebruers *et al.* [32] with  
128 a few modifications. The procedure was down-scaled and extended storage times,  
129 during which the protein population may undergo unwanted modifications, e.g. due to  
130 wheat endogenous enzymes, were avoided. TAXI-type proteins were bound to the  
131 first AC column, coupled with a GH family 11 *B. subtilis* xylanase. Isolation of XIP-  
132 and TLXI-type proteins was performed in a second affinity-based step, this time with  
133 an immobilized GH family 11 *A. niger* xylanase as biospecific ligand. Protein  
134 concentrations were estimated according to Bradford [33] with BSA as standard.  
135 A second, modified procedure for purification of XIs from wheat whole meal was  
136 performed to affirm or disaffirm the generation of artefacts during extraction and  
137 isolation. Complete Protease Inhibitor Cocktail (1 tablet/ 50 ml buffer) and pepstatin  
138 A (35 µg/ 50 ml buffer) were added to the aqueous extraction solution as well as to  
139 the eluates of the CEC column. Furthermore, all extraction and purification steps were  
140 performed at 7°C and in the shortest time period possible (~3 days).

141

#### 142 **2.4 2-DE and staining**

143 TCA-acetone pellets of crude wheat soluble proteins (see above) were dissolved in  
144 150 µl lysis buffer (7.0 M urea, 2.0 M thiourea, 4.0% CHAPS, 20 mM DTT, 0.5%  
145 IPG pH 6-11 buffer, trace of bromophenol blue) and the protein concentration was  
146 measured using the 2D-Quant-kit (GE Healthcare, Uppsala, Sweden) as described by  
147 the manufacturer. Affinity-purified XI fractions (see above) were desalted and  
148 concentrated to ca. 2.0 mg/ml by means of ultrafiltration using Vivaspin 15R  
149 concentrators with a molecular mass cut-off of 5,000 Da (Sartorius AG, Goettingen,



150 Germany). Forty microgram protein aliquots were fully denatured by addition of lysis  
151 buffer.

152 Immobiline Drystrips pH 6-11 (18×0.3×0.5 cm) were reswollen overnight in 340 µl  
153 Destreak rehydration solution (GE Healthcare) containing 0.5% IPG buffer. Samples  
154 were cup-loaded near the anode and focused at 20°C using the Ettan IPGphor II IEF  
155 unit (GE Healthcare). The running parameters for IEF were 500 V (120 min), 500-  
156 1000 V (60 min), 1000-10000 V (180 min), and 10000 V (55 min), reaching a total of  
157 at least 27 kVh. Prior to SDS-PAGE, the IPG-strips were reduced for 15 min at room  
158 temperature (RT) using an equilibration buffer (6.0 M urea, 50 mM Tris-HCl pH 8.8,  
159 2% SDS, 30% glycerol, trace of bromophenol blue) containing 65 mM DTT, followed  
160 by an alkylation step of 15 min at RT with the same buffer containing 135 mM  
161 iodoacetamide. The IPG strips were then transferred to 15% homogenous  
162 polyacrylamide (PAA) gels (25×20×0.1 cm) and SDS-PAGE was performed at 20°C  
163 using the Ettan Daltsix vertical electrophoresis system in conjunction with the Tris-  
164 glycine buffer system [34]. Protein entry was accomplished at 2 W/gel for 45 min,  
165 followed by separation at 17 W/gel for 4.5 h. 2-DE gels were stained with the  
166 sensitive CBB G-250 method as described by Candiano *et al.* [35] or using silver  
167 staining based on Blum *et al.* [36] and scanned via the ImageScanner II system with  
168 accompanying Labscan 5.00 software (GE Healthcare).

169 To selectively visualise the glycoproteins present in 2-DE gels a sequential  
170 fluorescence-based staining procedure, comprising the Pro-Q® Emerald 300  
171 Glycoprotein stain and the Sypro Ruby total protein stain (Invitrogen, Carlsbad, CA,  
172 USA) was applied according to the manufacturer's instructions.

173

## 174 **2.5 Protein identification by tandem mass spectrometric analysis**

175 Protein spots were picked manually from CBB stained gels, and trypsin-digested  
176 according to the method of Shevchenko *et al.* [37]. Tryptic digests were analyzed by  
177 LC-ESI-MS/MS on a LCQ Classic (Thermo Electron, San Jose, CA, USA) ion trap  
178 MS equipped with a nano-LC column switching system as described by Dumont *et al.*  
179 [38]. MS/MS data were searched against the Viridiplantae division of the GenBank  
180 non-redundant protein database using the Mascot (Matrix Sciences, London, U.K.)  
181 and against a custom database using the Sequest (Thermo Electron) algorithm. The  
182 latter contained all GenBank plant XI sequences as of 10 October 2007, as well as  
183 clustered XI-encoding EST sequences. In addition, recently submitted putative TAXI  
184 sequences were added to the custom database. The SEQUEST/MASCOT mass  
185 tolerance for parent and fragment ions were +3 and +1 Da, respectively.  
186 Carbamidomethylation of Cys and oxidation of Met, Trp and His were set as fixed  
187 and variable modifications, respectively. Maximally one missed cleavage was  
188 allowed, and the neutral loss of water and ammonia from b- and y-ions was taken into  
189 consideration. To allow detection of eventually truncated N- and C-termini, the  
190 custom database was subsequently N- and C-terminally ‘ragged’ using DBToolkit  
191 version 3.1 [39]. For every ‘parent’ sequence the ‘ragging’ process created a series of  
192 subsequences. From each  $n$ -th subsequence (with  $1 \leq n \leq 30$ ), the first  $n-1$  residues  
193 were removed from the N- and C-termini.

194

## 195 **2.6 C-terminal and *de novo* sequence analysis**

196 Cyanogen bromide (CNBr)-fragments were generated for C-terminal analysis [40].  
197 *De novo* sequence analysis of chemically derivatized peptides was carried out  
198 essentially as described previously [41]. Mass analysis was performed on an Applied  
199 Biosystems 4700 Proteomics Analyzer with TOF/TOF optics [42]. Samples were

200 prepared by spotting 1  $\mu$ l of a mixture of sample and matrix (7 mg/ml CHCA in 50%  
201 ACN containing 0.1% TFA) on a stainless steel (192-well) MALDI target plate and  
202 allowed to air-dry at RT. Prior to MALDI-MS analysis, the instrument was externally  
203 calibrated with a mixture of Angiotensin I, Glu-fibrino-peptide B, ACTH (1-17), and  
204 ACTH (18-39). For MS/MS experiments, the instrument was externally calibrated  
205 with fragments of Glu-fibrino-peptide.

206

## 207 **2.7 Immunoblot analysis**

208 Polyclonal antibodies (PABs), specifically interacting with TAXI-, XIP- or TLXI-type  
209 XIs, were obtained by rabbit immunisation as described by Beaugrand and co-workers  
210 [43]. Further purification of the PABs by AC with immobilised native TAXI-, XIP- or  
211 rTAXI-type inhibitors improved specificity. 2-DE separated proteins were  
212 electroblotted (16V, 40 min) onto an activated Protran (0.45  $\mu$ m pore size)  
213 nitrocellulose membrane (Schleicher and Schuell, Dassel, Germany) and probed with  
214 anti-TAXI, anti-XIP and anti-TLXI PABs as described before [43].

215

## 216 **2.8 Determination of apparent xylanase inhibitor activity**

217 Apparent XI activities of wheat whole meal fractions or run-through fractions of CEC  
218 and AC columns were determined colorimetrically with the Xylazyme AX method as  
219 described by Gebruers *et al.* [20]. Conversion of XI activities into inhibitor levels was  
220 described by Dornez *et al.* [44]. The levels of TAXI- and XIP-type inhibitors were  
221 measured using a specific GH family 11 *B. subtilis* xylanase and a GH family 10 *P.*  
222 *purpurogenum* xylanase, respectively.

223

## 224 **2.9 Chemical deglycosylation of xylanase inhibitors**

225 Affinity-purified and desalted XIs were lyophilized in small glass vials to create a  
226 moisture-free atmosphere for deglycosylation with trifluoromethanesulfonic acid  
227 (TFMS) [17, 45]. Briefly, dry sample aliquots (500 µg) were incubated (180 min) on  
228 ice with a pre-cooled 10.0% anisole in TFMS solution and neutralized by gradually  
229 adding droplets of a 60% pyridine solution, thereby keeping the samples at -15°C in a  
230 MeOH/dry ice bath. Prior to 2-DE, pellets were dissolved in lysis buffer (see above).

231

### 232 **2.10 Enzymatic dephosphorylation of xylanase inhibitors**

233 Affinity-purified and desalted XIs were dephosphorylated using broad spectrum λ-  
234 PPase. Forty microgram protein aliquots were prepared in 50 µl λ-PPase buffer (50  
235 mM Tris-HCl pH 7.8, 5.0 mM DTT) and incubated for 24 h at 30°C with 0 (negative  
236 control sample) and 800 units of enzyme in the presence of 2.0 mM MnCl<sub>2</sub>.  
237 Ovalbumin (GE Healthcare) and casein were treated in a similar way and used as  
238 positive control samples, while BSA was used as a negative control. After  
239 dephosphorylation, proteins were desalted and concentrated by means of ultrafiltration  
240 using Microcon YM-3 centrifugal filter units with molecular mass cut-off of 3,000 Da  
241 (Millipore, Billerica, MA, USA). Prior to SDS-PAGE and 2-DE analysis, proteins  
242 were dissolved in sample buffer (see below) and lysis buffer (see above), respectively.

243

### 244 **2.11 1-D gel electrophoresis and staining**

245 SDS-PAGE was performed on commercial 20% PAA gels using the PhastSystem unit  
246 (GE Healthcare). Proteins were denatured in sample buffer (10% glycerol, 62.5 mM  
247 Tris-HCl pH 6.8, 2% SDS (w/v), 5% 2-mercaptoethanol (v/v), trace of bromophenol  
248 blue). For serial detection of phosphoprotein and total protein profiles, Pro-Q®  
249 Diamond Phosphoprotein gel staining (Invitrogen) and subsequent silver staining were

250 performed according to the manufacturer's instructions. Phosphoproteins were  
251 visualised with a Typhoon 9400 laser fluorescence scanner (GE Healthcare) at an  
252 excitation wavelength of 532 nm and using a 560 nm long pass emission filter.

## 253 **3 RESULTS AND DISCUSSION**

### 254 **3.1 2-DE of wheat soluble seed proteins**

255 Since all three types of XIs are high-*pI* proteins [46], high-resolution separation of  
256 wheat seed proteins (cultivar Claire, Fig. 1) was realized in a linear alkaline pH-  
257 gradient of 6 to 11. SDS-PAGE was achieved on 15% homogenous PAA gels,  
258 covering a molecular mass range between 10 and 60 kDa, ideally suited for the  
259 separation of the three classes of XIs.

260 Evaluation of the 2-DE pattern (Image Master 2D-Platinum software, GE Healthcare)  
261 resulted in the detection of over a thousand spots. To reveal the presence and location  
262 of the three classes of XIs in this complex pattern of wheat seed proteins, 2D-gels  
263 were subjected to immunoblotting with PABs, specifically reacting with TAXI-, XIP-  
264 or TLXI-type XIs. Fig. 1 shows that the extraction/precipitation procedure and  
265 subsequent 2-DE analysis preserved the three classes of XIs, as immunostaining was  
266 observed for the 40 and 30 kDa polypeptides of TAXI-type proteins, as well as for  
267 XIP- and TLXI-type XIs. As expected, the 10 kDa C-terminal parts of the cleaved  
268 form of TAXI-type proteins escaped this pH-range, given their more acidic *pI*-values  
269 (*pI* 5.0-5.3) [20].

270 The large number of spots, detected with western blotting and probing with XI-  
271 specific PABs, was not anticipated. To reveal the large heterogeneity in XIs and, in  
272 addition to allow detection and identification of relatively low-abundant forms, a  
273 selective enrichment of the target proteins was performed.

274

### 275 **3.2 2-DE of isolated polymorphic wheat xylanase inhibitors**

#### 276 **3.2.1 Purification of the three types of wheat xylanase inhibitors**

277 To reduce the large number of non-inhibitor proteins present in wheat grain extracts  
278 while retaining all different forms of the three classes of XI-proteins, a selective,  
279 chromatographic pre-fractionation step was performed.  
280 TAXI-, XIP- and TLXI-type XIs were isolated from wheat whole meal extracts  
281 originating from three European wheat cultivars, selected for their distinct XI  
282 activities. TAXI and XIP levels, measured *in vitro* by the Xylazyme AX method, were  
283 110, 90 and 155 ppm, and 375, 300 and 325 ppm, for the Claire, Koch and Zohra  
284 cultivars, respectively. Following extraction and concentration by CEC, wheat whole  
285 meal extracts were applied on a series of two affinity columns. Only members of the  
286 TAXI inhibitor class were retained by the *B. subtilis* xylanase, while the *A. niger*  
287 xylanase bound the remaining two types of inhibitors.

288

### 289 **3.2.2 2-DE fingerprints of purified xylanase inhibitors**

290 For affinity-purified, desalted protein fractions, containing almost solely TAXI-type  
291 (Fig. 2A) or XIP-/TLXI-type (Fig. 3A) XIs, reproducible high-resolution spot  
292 fingerprints were obtained in the pH-gradient 6-11, and with SDS-PAGE on 15%  
293 PAA gels. Thus, TAXI-, XIP- as well as TLXI-type inhibitors exhibit a large  
294 variability in molecular mass and/or *pI* within a single wheat cultivar, as was expected  
295 from the western blot experiment. Moreover, despite some small differences between  
296 these 2-DE fingerprints (Figs. 2A and 3A) and the immunoblotted 2-DE patterns (Fig.  
297 1), possibly due to differences in inhibitor concentration or presence/absence of other  
298 wheat seed proteins, the overall spot patterns were very similar, validating the  
299 affinity-based purification.

300 For the spots identified as TAXI-type proteins (see paragraph 3.3.1), only small  
301 differences in molecular mass could be detected, while a large variation in *pI*-values

302 was visible (Fig. 2A). Estimated molecular masses were 45-46 kDa for the non-  
303 cleaved form and 32-33 kDa for the N-terminal polypeptides of processed TAXI-type  
304 proteins. These values are slightly higher than expected from their amino acid  
305 sequences. A few faint spots with lower molecular masses (41-44 kDa and 25-27  
306 kDa), were observed as well. They may have arisen from partial break-down of the  
307 TAXI protein, albeit without major structural changes to the active site as they still  
308 bind to the enzymes on the affinity columns. The non-processed form of TAXI-type  
309 proteins corresponded to spots with *pI*-values between ~7.5 and ~9.5, while the *pI*-  
310 range for the N-terminal polypeptides of the processed form varied between ~8.9 and  
311 9.5. In contrast to TAXI-type inhibitors, the spots, identified as XIP-type proteins (see  
312 paragraph 3.3.1), showed much greater variability in molecular mass (Fig. 3A). The  
313 2-DE pattern consisted of vertical rows of spots with molecular masses varying  
314 between 29 and 36 kDa, which were positioned at *pI*-values between ~7.2 and ~9.4.  
315 The same was true for the spots identified as TLXI proteins (see paragraph 3.3.1),  
316 except that there was only one row of spots at *pI* ~9.8 and within a molecular mass  
317 range of 18-21 kDa. As for TAXI-type inhibitors, a few weak spots of XIP-(iso)forms  
318 were visible at lower molecular masses.

319 Furthermore, the 2-DE patterns obtained for the polymorphic families of XIs, present  
320 in cultivar Claire, were very similar for the cultivars Koch (Figs. 2B and 3B) and  
321 Zohra (Figs. 2C and 3C). About 95% of all XI forms (matched in Image Master 2D-  
322 Platinum software) were found in the three cultivars. Spots 45-47 (Fig. 3A) from  
323 cultivar Claire were slightly shifted in cultivars Koch and Zohra, possibly because of  
324 variable post-translational modifications or (homoeo)allelic variation and, more  
325 exceptionally, the cultivar Zohra did not show spots near 18-21 kDa, which implies



326 that TLXI-type proteins are not present, or only present in undetectable amounts in  
327 this cultivar.

328

### 329 **3.3 Identification of affinity-purified proteins**

#### 330 **3.3.1 Xylanase inhibitor proteins**

331 Using LC-ESI-MS/MS most of the protein spots (Figs. 2A and 3A) were identified as  
332 XIs (Table 1, Supplementary Table 1). Moreover, an attempt was undertaken to  
333 distinguish between genetic variants, despite their limited differences in amino acid  
334 sequences.

335 Until recently, gene sequences of six TAXI variants have been published, i.e. *Taxi-Ia*  
336 (AJ438880) [21], *Taxi-Ib* (AJ697851), *Taxi-IIa* (AJ697849), *Taxi-IIb* (AJ697850)  
337 [22], *Taxi-III* (AB178471) and *Taxi-IV* (AB114628) [18]. In addition, six putative  
338 wheat TAXI-sequences, *Taxi-725ACCN* (EU082811), *Taxi-725ACC* (EU082810),  
339 *Taxi-725OS* (EU082812), *Taxi-602OS* (EU082813) *Taxi-801OS* (EU082814) and  
340 *Taxi-801NEW* (EU082815) were made available too.

341 In total, 24 spots were unequivocally (from 3 up to 20 non-redundant significant  
342 peptide hits per spot) identified as TAXI-type proteins (Table 1, Supplementary Table  
343 2). Among these, 13 spots correspond to full-length TAXI form A (Fig. 2A, spots 1-  
344 13), and 11 spots to the 30 kDa fragment of form B (Fig. 2A, spots 14-24). The  
345 conserved cleavage site separating the 30 and 10 kDa TAXI polypeptides is indicated  
346 in Fig. 4. The high amino acid sequence similarity among the TAXI variants and  
347 hence the limited amount of variant specific tryptic peptides (Fig. 4), however, often  
348 confounded the search engines Mascot and Sequest, thereby complicating the proper  
349 assignment of spectra to a specific TAXI variant. Therefore, TAXI variants were  
350 tentatively assigned by manually calculating the maximum number of significantly

351 scored, variant matching peptide hits in each spot. When not all peptides could be  
352 matched to a single variant, a second or third tentative assignment of the spectra to  
353 other TAXI variants was performed. In this way, all 847 significantly scored tandem  
354 MS spectra could be ascribed to minimally 4 out of 12 TAXI sequence variants,  
355 present in our customized database, being TAXI-Ia, TAXI-IIa, TAXI-IV and TAXI-  
356 725ACCN. The occurrence of the variant TAXI-IIb (one specific peptide hit) cannot  
357 be excluded because only a two amino acid difference exists between TAXI-IIb and  
358 TAXI-IV, resulting in just two detectable distinct tryptic peptides. The same is true  
359 for TAXI-725ACCN and TAXI-725ACC, for which eight differences in amino acids  
360 exist, giving rise to only five detectable distinct tryptic peptides. None of the TAXI-  
361 725ACC specific peptides was observed, however. They could all be accounted for as  
362 originating from TAXI-725ACCN. Tryptic peptides specific for TAXI-Ib or TAXI-  
363 III, which show 99.6% identity, were not found in the corresponding 2-DE spot  
364 patterns. To date, TAXI-Ib has only been produced recombinantly in *Pichia pastoris*  
365 [22], while *Taxi-III* transcripts were only demonstrated to occur in lemma, palea and  
366 leaves of the wheat plant after pathogen inoculation [18]. It should be noted that the  
367 presence of other highly similar TAXI sequence variants cannot be ruled out either.  
368 After all, our data show that single spots often contain different TAXI sequence  
369 variants, and that each TAXI variant occurs in several different spots (Table 1).  
370 Regarding the identification of XIP-type proteins, the situation was less complex  
371 (Table 1). Full-length gene sequences were already described for *Xip-I* (Q8L5C6) [23]  
372 and *Xip-III* (BAD99103) [19]. Most recently Takahashi-Ando and co-workers [47]  
373 revealed the existence of *Xip-R1* (BAF74363) and *Xip-R2* (BAF74364) genes. In our  
374 analyses, the presence of both XIP-I (Fig. 3A, spots 30, 32-51) and XIP-III (Fig. 3A,  
375 spots 25-29, 31) in the 2-DE pattern was confirmed, while none of the MS/MS spectra

376 could be matched to XIP-R1 or XIP-R2. The latter two XIP-type family members  
377 probably reside in wheat plant parts, other than the caryopsis, or occur under other  
378 (stress) conditions. In total, 27 spots were unequivocally determined as XIP proteins  
379 (Supplementary Table 3). For the third class of XIs, all observed spots (Fig. 3A, spots  
380 52-55) correspond to the only TLXI encoding gene sequence (Table 1) thus far  
381 identified in wheat [17].

382 Most of the XI forms migrated to positions in the 2-DE gel which were in agreement  
383 with their theoretical *pI*-values, e.g. TAXI-725ACCN and XIP-III forms, which have  
384 the lowest theoretical *pI*-values among the XI proteins, were situated close to the  
385 neutral part of the pH-range.

386 Most prominent in the identification of different genetic variants was the observation  
387 that the number of protein spots in the 2-DE patterns of all three classes of XIs highly  
388 exceeded the number of distinguished genetic variants. To check the possibility that  
389 the large variation was caused by proteolytic activity or other side reactions during the  
390 protein isolation, the extraction/purification of the three classes the XIs was carried  
391 out again for the cultivar Claire. This time a mixture of protease inhibitors was added  
392 and the temperature was reduced to prevent the formation of artificial products as  
393 much as possible. Comparison of the 2-DE fingerprints, acquired for the multiple  
394 (iso)forms of the three classes of XIs, didn't reveal differences between the outcomes  
395 of the standard and the modified purification procedure (results not shown), implying  
396 that no artefacts were produced either due to endogenous proteolytic activity or  
397 enzymatic side reactions. Hence, the large heterogeneity in inhibitor forms is most  
398 likely caused *in planta* by PTMs. It can not be excluded, however, that other XI gene  
399 sequences exist, which are thus far unknown because of the size and complexity of  
400 the hexaploid, not yet fully sequenced, wheat genome.

401 XIs in wheat grains thus are present as multiple forms, displaying charge- and  
402 molecular mass heterogeneity and, at least TAXI- and XIP-type XIs seem to be  
403 organized in multigene families. These observations fit well with their suggested role  
404 as plant defence-related proteins and are in line with observations on  
405 polygalacturonase inhibitors, which evolved as large families with specific  
406 recognition abilities against the many polygalacturonases produced by  
407 phytopathogenic fungi [24]. Thus far, different xylanase specificities of TAXI-I- and  
408 TAXI-II-type XIs have been demonstrated [20]. It is thus not unlikely that XIs too  
409 underwent a co-evolution with their pathogenic counterparts, resulting in the presence  
410 of a large heterogeneity in expressed forms, conferring enhanced resistance to  
411 multiple pathogens [48]. Igawa and co-workers [18] provided evidence for induced  
412 expression of *Taxi-III* and *Taxi-IV* in lemma/palea or leaves upon infection with *F.*  
413 *graminearum* and *E. graminis*, while expression of *Taxi-I* is only up-regulated in  
414 response to abiotic stress. Furthermore it has been demonstrated that *Xip-I* and *Xip-*  
415 *R1*, but not *Xip-III* and *Xip-R2*, are strongly transcribed in infected wheat leaves,  
416 though this appears to be pathogen-dependent [19, 47]. Wounding, as well as  
417 treatment of leaves with methyl jasmonate, also enhance the expression of *Xip-I* [19].  
418 Accordingly, it is hypothesized that, within the large polymorphism, some XI forms  
419 are basal pre-existing defence-related proteins, while others have a more specialized  
420 protective role triggered by specific biotic or abiotic stimuli [19, 47].

421

### 422 **3.3.2 Non-xylanase inhibitor proteins**

423 From Fig. 2A it can be deduced that, next to spots corresponding to TAXI-type  
424 inhibitors, the XI protein preparation also contained some impurities, co-purified on  
425 the *B. subtilis* affinity matrix (Supplementary Table 1). Among these, a bifunctional

426  $\alpha$ -amylase inhibitor, a class II chitinase, LMW glutenin subunits, a thaumatin-like  
427 protein TLP7,  $\beta$ -glucosidases and some unidentified proteins were coupled, probably  
428 by non-specific interactions. In the area near neutral *pI* (6.0-7.0) and low molecular  
429 mass (< 18 kDa), a small group of intense spots could be matched by MS/MS to  $\alpha$ -  
430 amylase inhibitors (Table 1). Their high abundance in the purified XI fraction was  
431 surprising. In contrast to other impurities present, the pattern of the  $\alpha$ -amylase  
432 inhibitors remained unaltered, irrespective of purification scheme or wheat cultivar  
433 (Fig. 2). It is not yet clear whether these proteins interact with the *B. subtilis* xylanase  
434 or with TAXI-type inhibitors, and whether they possess any XI activity in addition to  
435 their  $\alpha$ -amylase inhibitor activity.

436

### 437 **3.4 Post-translational modifications**

438 The high multiplicity of spots, identified as the same gene product but differing in  
439 molecular mass and/or *pI*, supports the occurrence of different PTMs for the three  
440 types of XIs, independent of wheat cultivar. In order to gain more insight into the  
441 post-translational heterogeneity of the polymorphic families of wheat XIs, some of  
442 the most commonly occurring PTMs were examined.

443

#### 444 **3.4.1 Spots with a different molecular mass and the same *pI***

445 XIP- and TLXI-type XIs show vertical rows of spots in their 2-DE patterns, indicative  
446 for varying degrees of glycosylation, whereas less variation in molecular mass is seen  
447 for TAXI-type proteins. TAXI-type XIs have a predicted N-glycosylation site at  
448 Asn<sup>105</sup> (TAXI-Ia and TAXI-725ACCN) or Asn<sup>107</sup> (TAXI-IV/IIb and TAXI-IIa) (Fig.  
449 4) [48]. XIP-I/XIP-III and TLXI have a Asn-X-Ser/Thr motif at positions 89 and 95,  
450 respectively [17, 49].

451 To reveal the non-glycosylated ‘parent’ 2-DE pattern for the three types of XIs,  
452 chemical deglycosylation of the affinity-purified proteins was accomplished using  
453 TFMS. As expected for XIP- and TLXI-type proteins (Fig. 5B), the vertical trains of  
454 spots disappeared due to the acid treatment. For TAXI-type proteins (Fig. 5A) no  
455 differences in molecular mass were seen, however, a noticeable shift in *pI* was  
456 observed upon deglycosylation. This was even more so the case for XIP- and TLXI-  
457 type proteins. One reason for this shift towards the cathode upon deglycosylation may  
458 be the removal of negatively charged sialic acid residues which are possibly build-in  
459 as part of the complex carbohydrate structure [51]. A pathway for sialylation was only  
460 recently discovered in plants [50] and, moreover, for TLXI, the incorporation of one  
461 sialic acid residue in the glycan structure has been described [17]. Although it can not  
462 be taken for granted, it has been demonstrated that the effect of TFMS, in the  
463 presence of anisole as scavenger, is sufficiently specific, in the sense that the protein  
464 backbone and the PTMs, other than glycosylation are stable during the treatment [45,  
465 52].

466 To complement the above results, TAXI- and XIP-/TLXI-type proteins were, before  
467 and after deglycosylation, stained with the fluorescent Pro-Q Emerald 300  
468 glycoprotein stain. The small signal for TAXI-type proteins (Fig. 6A) disappeared  
469 upon deglycosylation, while the intense glycoprotein signal of XIP- and TLXI-type  
470 inhibitors (Fig. 6B) remained only slightly visible (result not shown). The residual  
471 fluorescence may have been due to the presence of N-acetylhexosamine of N-linked  
472 glycans that escapes removal by TFMS [45]. Post-staining with Sypro Ruby  
473 confirmed the presence of XI spots in gels giving no Pro-Q Emerald signal.

474

#### 475 **3.4.2 Spots with a different *pI* and the same molecular mass**

476 In the case of TAXI- (Fig. 2) and XIP-type (Fig. 3) inhibitors, all genetic variants,  
477 identified by MS, emerge as multiple spots with distinct *pI*-values. Conversely, TLXI-  
478 type (Fig. 3) proteins were not modified in a way that alters the *pI*. It could thus be  
479 postulated that at least some of the TAXI- and XIP-type XIs are phosphorylated  
480 whereas TLXI-type inhibitors are not.

481 For this purpose, prior to 2-DE, purified TAXI- and XIP-/TLXI-type XIs were treated  
482 with  $\lambda$ PPase, which acts on all currently known phosphorylated amino acid residues.  
483 The dephosphorylated protein patterns for TAXI-, as well as XIP- and TLXI-type XIs  
484 (results not shown), were identical to the ones obtained before. This result was  
485 confirmed by comparison of dephosphorylated and intact XIs with phosphorylated  
486 (casein and ovalbumin) and non-phosphorylated (BSA) control proteins using 1D-  
487 SDS-PAGE and Pro-Q-Diamond phosphostaining (Fig. 7A), followed by silver  
488 staining (Fig. 7B). From these experiments, we can conclude that phosphorylation  
489 does not contribute to the complexity of the XI spot patterns, in particular to  
490 differences in *pI*. Modifications such as acetylation, methylation, deamidation and  
491 sialylation all may give rise to cathodic shifts in 2-DE. Examination of these options  
492 will require more extensive biochemical analyses.

493

#### 494 **3.4.3 Micro-heterogeneity at the C-or N-terminal end of the amino acid chain**

495 Terminal truncation was investigated by including systematically N- or C-terminally  
496 shortened TAXI and XIP sequence variants in the Sequest database. This way,  
497 deletions of 1 or 2 amino acids at the TAXI N-terminus were frequently observed by  
498 ESI-MS/MS (Supplementary Table 2). In contrast, C-terminal peptides, if observed,  
499 were untruncated.

500 To further verify whether the different XI-forms are processed *in planta*, CNBr-  
501 fragments from multiple spots were generated and analyzed by MALDI-MS and  
502 MS/MS analysis [34]. As an example, MS analysis of the CNBr-fractions in spot 2  
503 (Fig. 2A) reveals three peptides with respective  $m/z$  values of 1574.85, 1849.08 and  
504 2160.22 Da. The first two correspond to internal CNBr-fragments of the TAXI-  
505 725ACCN isoform (both with a homoserinelactone derivative,  $\Delta m = -48$  Da) while  
506 the mass of the fragment at  $m/z$  2160.22 is in full agreement with the theoretical mass  
507 of the C-terminal fragment Glu364-Leu382 (calculated molecular mass 2159.14 Da).  
508 In spot 3 (Fig. 2A), three CNBr-fragments at  $m/z$  values of 1791.05, 2254.37 and  
509 2160.21 Da were also observed. The two former represent internal fragments  
510 indicative for TAXI-Ia (Fig. 4), while the latter coincides with the intact C-terminus.  
511 The C-termini of some TAXI proteins were also identified by *de novo* sequence  
512 analysis of chemically derivatized tryptic peptides. As an example, in spot 1 and 2,  
513 both identified as TAXI-725ACCN, the C-terminal tryptic peptide,  
514 LGFSRLPHFTGCGGL (Leu368-Leu382) (Fig. 4) was seen by MS/MS analysis.  
515 CNBr-fragments were also derived for a number of the XIP-type proteins before and  
516 after deglycosylation, since MS often fails to detect glycosylated peptides. In spots 34  
517 and 44 (Fig. 3A), two main signals at  $m/z$  2793.3 and 3037.4 Da were observed after  
518 CNBr-cleavage. These two fragments correspond to the C- and N-terminal fragments  
519 of the XIP-I-isoform, as deduced from MS/MS analysis and partial N-terminal  
520 sequence analysis, respectively (results not shown). After deglycosylation, the same  
521  $m/z$  values of the XIP-I-isoform were observed in spots 2-4 (Fig. 5B), with an  
522 additional fragment at 1264.6 Da. MS/MS analysis of the latter indicated that it  
523 contains the N-terminal sequence, probably generated by a non-specific cleavage.  
524 This N-terminal fragment was also present in spot 1 (Fig. 5B) with a satellite peak at



525  $m/z$  1344.5 ( $\Delta M$  80 Da). Together, this illustrates that neither C- nor N-terminal  
526 processing is responsible for the different horizontal position of the XI spots which  
527 share an identical MS identification.

528 **CONCLUDING REMARKS**

529 In the present study, 2-DE and subsequent tandem MS analysis were successfully  
530 used to reveal the presence of complex polymorphic XI families in wheat grain and,  
531 in addition, to gain insight in the genetic variability present. Moreover, this is the first  
532 paper with a simultaneous emphasis on the three XI classes, currently found in wheat.  
533 Thanks to a refined pre-fractionation step and the availability of improved basic pH-  
534 gradient protocols, it was possible to effectively focus on a small, but from a plant  
535 physiological and a wheat processing point of view, very interesting part of the wheat  
536 grain proteome.

537 Although multiple XI genes were already available in public databases, we were able  
538 to show that not all of them are actually expressed in wheat grains, or at least not to  
539 the same extent. For instance, no variant specific tryptic peptides of TAXI-III/Ib or  
540 XIP-R1/R2 were found, while the putative TAXI-725ACCN and XIP-III variants, for  
541 which it was not yet known whether expression actually occurred in the mature wheat  
542 caryopsis, could be identified in several (major) spots. This underlines the need for  
543 integration of data on genomic and proteomic levels. The proteomic approach also  
544 enabled us to investigate some ubiquitous PTMs. Glycosylation is responsible for the  
545 variation in molecular mass, observed for XIP- and TLXI-type proteins. Some genetic  
546 variants of TAXI- and XIP-type proteins display differences in *pI*, which could not be  
547 attributed to phosphorylation or processed C- or N-termini. The existence of yet  
548 unknown wheat XI gene sequences can not be excluded.

549 When looking down the road, the obtained results, including the 2-DE fingerprints of  
550 TAXI-, XIP-, and TLXI-type proteins, will be instrumental in exploring the temporal  
551 and spatial distribution of XIs in wheat grains by analyzing successive developmental/  
552 germination stages and different milling fractions or kernel tissues, respectively.

553 Additionally, 2-DE analysis of wheat, infected with ubiquitous cereal pathogens, e.g.  
554 *F. graminearum*, can provide useful information on the physiological role of TAXI-,  
555 XIP-, and TLXI-type (iso)forms in plant defence. More research on such proteins,  
556 important for plant resistance, can pave the way for the development of efficient  
557 strategies in environment-sound plant protection.

558 In conclusion, next to providing insight in the variability of polymorphic XI families,  
559 this work contributes to a better understanding of the link between XI proteins and XI  
560 genes, effectively expressed in wheat. It further provides a strong basis for the  
561 analysis of the temporal and spatial distribution of XIs in wheat and of the presumed  
562 physiological role of TAXI-, XIP-, and TLXI-type (iso)forms in plant defence.

563 **ACKNOWLEDGEMENTS**

564 *The authors acknowledge the 'Instituut voor de aanmoediging van Innovatie door*  
565 *Wetenschap en Technologie in Vlaanderen' (I.W.T., Brussels, Belgium) for their*  
566 *financial support. Kurt Gebruers and Bart Samyn are postdoctoral fellows of the*  
567 *Fund for Scientific Research-Flanders (F.W.O., Flanders, Belgium). The authors*  
568 *would like to thank Gert Raedschelders for providing access to additional, putative XI*  
569 *gene sequences and critical reading.*

570 **REFERENCES**

- 571 [1] Biely, P., Vrsanska, M., Kucar, S., in: Visser, J., Beldman, G., Kusters-van  
572 Someren, M. A., Voragen, A. G. J. (Eds.), *Xylans and xylanases*, Elsevier Science  
573 Publishers, Amsterdam 1992, pp. 81-94.
- 574 [2] Henrissat, B., A Classification of Glycosyl Hydrolases Based on Amino-Acid-  
575 Sequence Similarities, *Biochem. J.* 1991, *280*, 309-316.
- 576 [3] Simpson, D. J., Fincher, G. B., Huang, A. H. C., Cameron-Mills, V., Structure and  
577 function of cereal and related higher plant (1 -> 4)-beta-xylan endohydrolases, *J.*  
578 *Cereal Sci.* 2003, *37*, 111-127.
- 579 [4] Giesbert, S., Lepping, H. B., Tenberge, K. B., Tudzynski, P., The xylanolytic  
580 system of *Claviceps purpurea*: Cytological evidence for secretion of xylanases in  
581 infected rye tissue and molecular characterization of two xylanase genes,  
582 *Phytopathology* 1998, *88*, 1020-1030.
- 583 [5] Kang, Z., Buchenauer, H., Ultrastructural and cytochemical studies on cellulose,  
584 xylan and pectin degradation in wheat spikes infected by *Fusarium culmorum*, *J.*  
585 *Phytopath.* 2000, *148*, 263-275.
- 586 [6] Wanjiru, W. M., Kang, Z. S., Buchenauer, H., Importance of cell wall degrading  
587 enzymes produced by *Fusarium graminearum* during infection of wheat heads, *Eur. J.*  
588 *Plant Pathol.* 2002, *108*, 803-810.
- 589 [7] Brito, N., Espino, J. J., Gonzalez, C., The endo-beta-1,4-xylanase xyn11A is  
590 required for virulence in *Botrytis cinerea*, *Mol. Plant-Microbe Interact.* 2006, *19*, 25-  
591 32.
- 592 [8] Christov, L. P., Szakacs, G., Balakrishnan, H., Production, partial characterization  
593 and use of fungal cellulase-free xylanases in pulp bleaching, *Process Biochem.* 1999,  
594 *34*, 511-517.

- 595 [9] Courtin, C. M., Delcour, J. A., Arabinoxylans and endoxylanases in wheat flour  
596 bread-making, *J. Cereal Sci.* 2002, 35, 225-243.
- 597 [10] Christophersen, C., Andersen, E., Jakobsen, T. S., Wagner, P., Xylanases in  
598 wheat separation, *Starch-Starke* 1997, 49, 5-12.
- 599 [11] Debyser, W., Derdelinckx, G., Delcour, J. A., Arabinoxylan and arabinoxylan  
600 hydrolysing activities in barley malts and worts derived from them, *J. Cereal Sci.*  
601 1997, 26, 67-74.
- 602 [12] Bedford, M. R., Schulze, H., Exogenous enzymes for pigs and poultry, *Nutr. Res.*  
603 *Rev.* 1998, 11, 91-114.
- 604 [13] Chivasa, S., Simon, W. J., Yu, X. L., Yalpani, N., Slabas, A. R., Pathogen  
605 elicitor-induced changes in the maize extracellular matrix proteome, *Proteomics*  
606 2005, 5, 4894-4904.
- 607 [14] Di, C. X., Zhang, M. X., Xu, S. J., Cheng, T., An, L. Z., Role of  
608 polygalacturonase-inhibiting protein in plant defense, *Crit. Rev. Microbiol.* 2006, 32,  
609 91-100.
- 610 [15] Debyser, W., Derdelinckx, G., Delcour, J. A., Arabinoxylan solubilization and  
611 inhibition of the barley malt xylanolytic system by wheat during mashing with wheat  
612 wholemeal adjunct: Evidence for a new class of enzyme inhibitors in wheat, *J. Am.*  
613 *Soc. Brew. Chem.* 1997, 55, 153-156.
- 614 [16] McLauchlan, W. R., Garcia-Conesa, M. T., Williamson, G., Roza, M., *et al.*, A  
615 novel class of protein from wheat which inhibits xylanases, *Biochem. J.* 1999, 338,  
616 441-446.
- 617 [17] Fierens, E., Rombouts, S., Gebruers, K., Goesaert, H., *et al.*, TLXI, a novel type  
618 of xylanase inhibitor from wheat (*Triticum aestivum*) belonging to the thaumatin  
619 family, *Biochem. J.* 2007, 403, 583-591.

620 [18] Igawa, T., Ochiai-Fukuda, T., Takahashi-Ando, N., Ohsato, S., *et al.*, New  
621 TAXI-type xylanase inhibitor genes are inducible by pathogens and wounding in  
622 hexaploid wheat, *Plant Cell Physiol.* 2004, *45*, 1347-1360.

623 [19] Igawa, T., Tokai, T., Kudo, T., Yamaguchi, I., Kimura, M., A wheat xylanase  
624 inhibitor gene, Xip-I, but not Taxi-I, is significantly induced by biotic and abiotic  
625 signals that trigger plant defense, *Biosci. Biotechnol. Biochem.* 2005, *69*, 1058-1063.

626 [20] Gebruers, K., Debyser, W., Goesaert, H., Proost, P., *et al.*, Triticum aestivum L.  
627 endoxylanase inhibitor (TAXI) consists of two inhibitors, TAXI I and TAXI II, with  
628 different specificities, *Biochem. J.* 2001, *353*, 239-244.

629 [21] Fierens, K., Brijs, K., Courtin, C. M., Gebruers, K., *et al.*, Molecular  
630 identification of wheat endoxylanase inhibitor TAXI-I-1, member of a new class of  
631 plant proteins, *FEBS Lett.* 2003, *540*, 259-263.

632 [22] Raedschelders, G., Fierens, K., Sansen, S., Rombouts, S., *et al.*, Molecular  
633 identification of wheat endoxylanase inhibitor TAXI-II and the determinants of its  
634 inhibition specificity, *Biochem. Biophys. Res. Commun.* 2005, *335*, 512-522.

635 [23] Elliott, G. O., Hughes, R. K., Juge, N., Kroon, P. A., Williamson, G., Functional  
636 identification of the cDNA coding for a wheat endo-1,4-beta-D-xylanase inhibitor,  
637 *FEBS Lett.* 2002, *519*, 66-70.

638 [24] Stotz, H. U., Bishop, J. G., Bergmann, C. W., Koch, M., *et al.*, Identification of  
639 target amino acids that affect interactions of fungal polygalacturonases and their plant  
640 inhibitors, *Physiol. Mol. Plant Pathol.* 2000, *56*, 117-130.

641 [25] Trogh, I., Sorensen, J. F., Courtin, C. M., Delcour, J. A., Impact of inhibition  
642 sensitivity on endoxylanase functionality in wheat flour breadmaking, *J. Agric. Food*  
643 *Chem.* 2004, *52*, 4296-4302.

644 [26] Frederix, S. A., Courtin, C. M., Delcour, J. A., Substrate selectivity and inhibitor  
645 sensitivity affect xylanase functionality in wheat flour gluten-starch separation, *J.*  
646 *Cereal Sci.* 2004, *40*, 41-49.

647 [27] Courtin, C. M., Gys, W., Gebruers, K., Delcour, J. A., Evidence for the  
648 involvement of arabinoxylan and xylanases in refrigerated dough syruing, *J. Agric.*  
649 *Food Chem.* 2005, *53*, 7623-7629.

650 [28] Juge, N., Svensson, B., Proteinaceous inhibitors of carbohydrate-active enzymes  
651 in cereals: implication in agriculture, cereal processing and nutrition, *J. Sci. Food*  
652 *Agric.* 2006, *86*, 1573-1586.

653 [29] Sørensen, J. F., Sibbesen, O., Mapping of residues involved in the interaction  
654 between the *Bacillus subtilis* xylanase A and proteinaceous wheat xylanase inhibitors,  
655 *Prot. Eng. Des. Sel.* 2006, *19*, 205-210.

656 [30] Bourgois, T. M., Nguyen, D. V., Sansen, S., Rombouts, S., *et al.*, Targeted  
657 molecular engineering of a family 11 endoxylanase to decrease its sensitivity towards  
658 *Triticum aestivum* endoxylanase inhibitor types, *J. Biotechnol.* 2007, *130*, 95-105.

659 [31] Sørensen, J. F., Kragh, K. M., Sibbesen, O., Delcour, J. A., *et al.*, Potential role  
660 of glycosidase inhibitors in industrial biotechnological applications, *Biochim.*  
661 *Biophys. Acta* 2004, *1696*, 275-287.

662 [32] Gebruers, K., Brijs, K., Courtin, C. M., Goesart, H., *et al.*, Affinity  
663 chromatography with immobilised endoxylanases separates TAXI- and XIP-type  
664 endoxylanase inhibitors from wheat (*Triticum aestivum* L.), *J. Cereal Sci.* 2002, *36*,  
665 367-375.

666 [33] Bradford, M. M., A rapid and sensitive method for the quantitation of microgram  
667 quantities of protein utilizing the principle of protein-dye binding, *Anal. Biochem.*  
668 1976, *72*, 248-254.



669 [34] Laemmli, U. K., Cleavage of structural proteins during the assembly of the head  
670 of bacteriophage T4, *Nature* 1970, 227, 680-685.

671 [35] Candiano, G., Bruschi, M., Musante, L., Santucci, L., *et al.*, Blue silver: A very  
672 sensitive colloidal Coomassie G-250 staining for proteome analysis, *Electrophoresis*  
673 2004, 25, 1327-1333.

674 [36] Blum, H., Beier, H., Gross, H. J., Improved silver staining of plant-proteins,  
675 RNA and DNA in polyacrylamide gels, *Electrophoresis* 1987, 8, 93-99.

676 [37] Shevchenko, A., Tomas, H., Havlis, J., Olsen, J. V., Mann, M., In-gel digestion  
677 for mass spectrometric characterization of proteins and proteomes, *Nat. Protoc.* 2006,  
678 1, 2856-2860.

679 [38] Dumont, D., Noben, J. P., Raus, J., Stinissen, P., Robben, J., Proteomic analysis  
680 of cerebrospinal fluid from multiple sclerosis patients, *Proteomics* 2004, 4, 2117-  
681 2124.

682 [39] Martens, L., Vandekerckhove, J., Gevaert, K., DBToolkit: processing protein  
683 databases for peptide-centric proteomics, *Bioinformatics* 2005, 21, 3584-3585.

684 [40] Samyn, B., Sergeant, K., Castanheira, P., Faro, C., Van Beeumen, J., A new  
685 method for C-terminal sequence analysis in the proteomic era, *Nat. Meth.* 2005, 2,  
686 193-200.

687 [41] Sergeant, K., Samyn, B., Debyser, G., Van Beeumen, J., De novo sequence  
688 analysis of N-terminal sulfonated peptides after in-gel guanidination, *Proteomics*  
689 2005, 5, 2369-2380.

690 [42] Samyn, B., Sergeant, K., Van Beeumen, J., A method for C-terminal sequence  
691 analysis in the proteomic era (proteins cleaved with cyanogen bromide), *Nat. Protoc.*  
692 2006, 1, 318-323.

693 [43] Beaugrand, J., Gebruers, K., Ververken, C., Fierens, E., *et al.*, Antibodies against  
694 wheat xylanase inhibitors as tools for the selective identification of their homologues  
695 in other cereals, *J. Cereal Sci.* 2006, *44*, 59-67.

696 [44] Dornez, E., Joye, I. J., Gebruers, K., Delcour, J. A., Courtin, C. M., Wheat-  
697 kernel-associated endoxylanases consist of a majority of microbial and a minority of  
698 wheat endogenous endoxylanases, *J. Agric. Food Chem.* 2006, *54*, 4028-4034.

699 [45] Edge, A. S. B., Deglycosylation of glycoproteins with trifluoromethanesulphonic  
700 acid: elucidation of molecular structure and function, *Biochem. J.* 2003, *376*, 339-350.

701 [46] Goesaert, H., Elliott, G., Kroon, P. A., Gebruers, K., *et al.*, Occurrence of  
702 proteinaceous endoxylanase inhibitors in cereals, *Biochim. Biophys. Acta* 2004, *1696*,  
703 193-202.

704 [47] Takahashi-Ando, N., Inaba, M., Ohsato, S., Igawa, T., *et al.*, Identification of  
705 multiple highly similar XIP-type xylanase inhibitor genes in hexaploid wheat,  
706 *Biochem. Biophys. Res. Commun.* 2007, *360*, 880-884.

707 [48] Sansen, S., De Ranter, C. J., Gebruers, K., Brijs, K., *et al.*, Structural basis for  
708 inhibition of *Aspergillus niger* xylanase by *Triticum aestivum* xylanase inhibitor-I, *J.*  
709 *Biol. Chem.* 2004, *279*, 36022-36028.

710 [49] Payan, F., Flatman, R., Porciero, S., Williamson, G., *et al.*, Structural analysis of  
711 xylanase inhibitor protein I (XIP-I), a proteinaceous xylanase inhibitor from wheat  
712 (*Triticum aestivum*, var. Soisson), *Biochem. J.* 2003, *372*, 399-405.

713 [50] Shah, M. M., Fujiyama, K., Flynn, C. R., Joshi, L., Sialylated endogenous  
714 glycoconjugates in plant cells, *Nat. Biotechnol.* 2003, *21*, 1470-1471.

715 [51] Kleinert, P., Kuster, T., Arnold, D., Jaeken, J., *et al.*, Effect of glycosylation on  
716 the protein pattern in 2-D-gel electrophoresis, *Proteomics* 2007, *7*, 15-22.

717 [52] Horvath, E., Edwards, A. M., Bell, J. C., Braun, P. E., Chemical Deglycosylation  
718 on a Micro-Scale of Membrane-Glycoproteins with Retention of Phosphoryl-Protein  
719 Linkages, *J. Neurosci. Res.* 1989, 24, 398-401.

720 **FIGURE CAPTIONS**

721 **Figure 1.** Silver stained 2-DE pattern (pH 6-11; 15% PAA gel) of low salt  
722 extractable wheat seed proteins (cultivar Claire, 350 µg). Rectangles represent  
723 particular regions containing the three types of XIs, visualised by western blotting and  
724 probing of membranes with specific anti-TAXI, anti-XIP or anti-TLXI PABs.

725

726 **Figure 2.** Colloidal CBB stained 2-DE patterns (pH 6-11; 15% PAA gels) of TAXI-  
727 type XIs (40 µg) purified from the wheat cultivars Claire (A), Koch (B) and Zohra  
728 (C). Numbered spots (A) were excised and analysed by LC-ESI-MS/MS (Table 1 and  
729 Supplementary Table 1).

730

731 **Figure 3.** Colloidal CBB stained 2-DE patterns (pH 6-11; 15% PAA gels) of XIP-  
732 and TLXI-type XIs (40 µg) purified from the wheat cultivars Claire (A), Koch (B)  
733 and Zohra (C). Numbered spots (A) were excised and analysed by LC-ESI-MS/MS  
734 (Table 1 and Supplementary Table 1).

735

736 **Figure 4.** Amino acid sequence alignment of TAXI-type XIs, without signal  
737 sequence (Clustal W, EBI, default parameters). (✓) indicates the conserved cleavage  
738 site separating the 30 and 10 kDa TAXI polypeptides. Underlined amino acids are  
739 LC-ESI-MS/MS sequenced peptide fragments (in agreement with Supplementary  
740 Table 2). CNBr-fragments are indicated in italics.

741

742 **Figure 5.** Colloidal CBB stained 2-DE patterns (pH 6-11; 15% PAA gels) of  
743 chemically deglycosylated TAXI-type (A) and XIP-/TLXI-type XIs (B) (cultivar  
744 Claire, 40 µg). Arrows indicate the shift in pI after deglycosylation, compared to the

745 original 2-DE patterns (Figs. 2A and 3A). Numbered spots (1-4) were submitted to C-  
746 terminal analysis.

747

748 **Figure 6.** 2-DE patterns (pH 6-11; 15% PAA gels) after staining with the fluorescent  
749 Pro-Q Emerald 300 glycoprotein gel stain, showing glycosylated proteins in TAXI-  
750 type (A) and XIP-type XIs (B) of wheat cultivar Claire (40 µg).

751

752 **Figure 7.** SDS-PAGE profile (under reducing conditions) of XI proteins, stained with  
753 Pro-Q Diamond phosphoprotein gel stain (A) and subsequently, using the sensitive  
754 silver staining (B) procedure. Casein and ovalbumin were used as positive control  
755 samples, while BSA was applied as a negative control. TAXI-type XIs (0.4 µg, 1);  
756 XIP/TLXI-type XIs (1.0 µg, 2); TLXI-type XIs (0.4 µg, 3); casein (0,4 µg, 4);  
757 ovalbumin (0,4 µg, 5); BSA (0,4 µg, 6).

**Table 1.** Tandem MS identification of spots, excised from 2-DE gels (pH 6-11; 15% PAA gels) of affinity-purified proteins originating from whole meal of wheat cultivar Claire.

Spot ID <sup>a</sup>	GenBank ID	Species	Protein Name	Theor. MW	Theor. pI
<b>TAXI-type xylanase inhibitors (40 kDa polypeptides)<sup>b</sup></b>					
1-2	EU082811	<i>Triticum aestivum</i>	TAXI-725ACCN	39.1	7.6
3,5	AJ438880	<i>Triticum aestivum</i>	TAXI-Ia	38.8	8.2
4,6-8	AB114628	<i>Triticum aestivum</i>	TAXI-IV	39.7	8.6
9-10	AJ697849	<i>Triticum aestivum</i>	TAXI-IIa	40.3	8.4
11-13	AB114628/AJ697850	<i>Triticum aestivum</i>	TAXI-IV/TAXI-IIb	39.7/40.3	8.6/8.4
<b>TAXI-type xylanase inhibitors (30 kDa polypeptides)<sup>b</sup></b>					
14-19,23-24	EU082811	<i>Triticum aestivum</i>	TAXI-725ACCN	27.0	8.6
20-21	AJ438880	<i>Triticum aestivum</i>	TAXI-Ia	26.9	8.7
22	AB114628	<i>Triticum aestivum</i>	TAXI-IV	27.0	9.0
<b>XIP-type xylanase inhibitors<sup>c</sup></b>					
25-29,31	AB204556	<i>Triticum aestivum</i>	XIP-III	30.5	6.9
30, 32-51	Q8L5C6	<i>Triticum aestivum</i>	XIP-I	30.3	8.3
<b>TLXI-type xylanase inhibitors<sup>d</sup></b>					
52-55	AJ786601	<i>Triticum aestivum</i>	TLXI	15.6	8.4
<b><math>\alpha</math>-amylase inhibitors<sup>d</sup></b>					
56-57	CAA35597	<i>Triticum aestivum</i>	$\alpha$ -amylase inhibitor CM3	18.2	7.4
58	AAV39518	<i>Triticum aestivum</i>	0.19 dimeric $\alpha$ -amylase inhibitor	13.3	6.7
59	CAA35598	<i>Triticum aestivum</i>	$\alpha$ -amylase inhibitor CM1	15.5	7.5
60	AAV39519	<i>Triticum aestivum</i>	0.19 dimeric $\alpha$ -amylase inhibitor	13.2	6.5
61	CAA39099	<i>Triticum turgidum</i>	$\alpha$ -amylase inhibitor CM2	15.5	6.9

a) Spot ID as indicated in Figs. 2A and 3A.

b) TAXI variants, tentatively assigned by manually calculating the maximal number of significantly scored, variant matching peptide hits in each spot (see Supplementary Table 2).

c) XIP variants, tentatively assigned by manually calculating the maximal number of significantly scored, variant matching peptide hits in each spot (see Supplementary Table 3).

d) Significantly scored peptides and Sequest/Mascot hits listed in Supplementary Table 1. Sequest cross correlation score  $\geq 3.5$  for triply charged peptide ions; Sequest cross correlation score  $\geq 2.5$  for doubly charged peptide ions; Sequest cross correlation score  $\geq 1.8$  for singly charged peptide ions; Mascot Expect value  $\leq 0.05$ .

Figure 1.

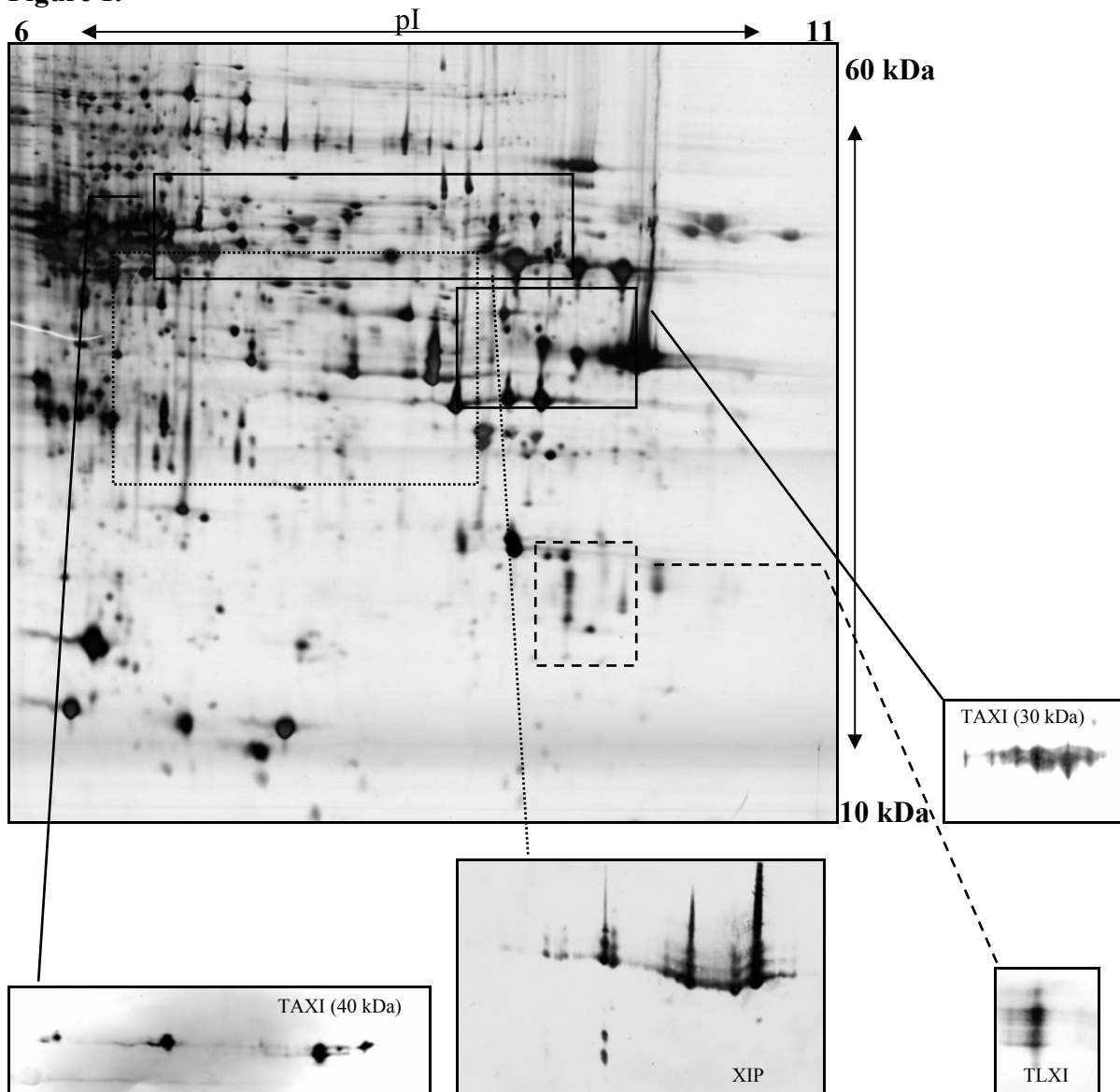


**Figure 2.**

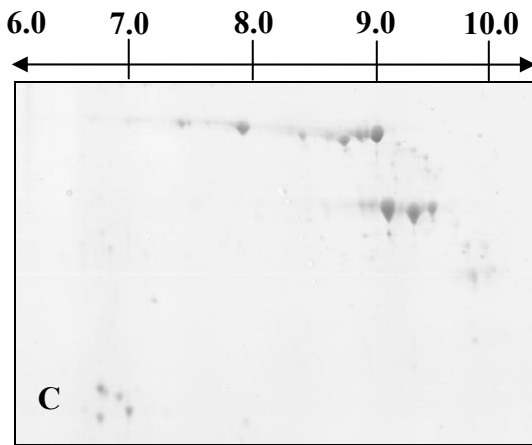
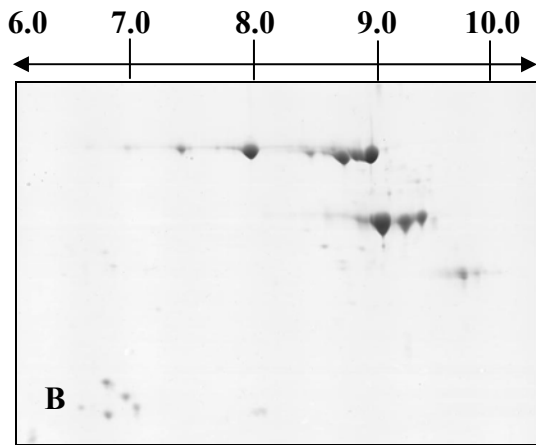
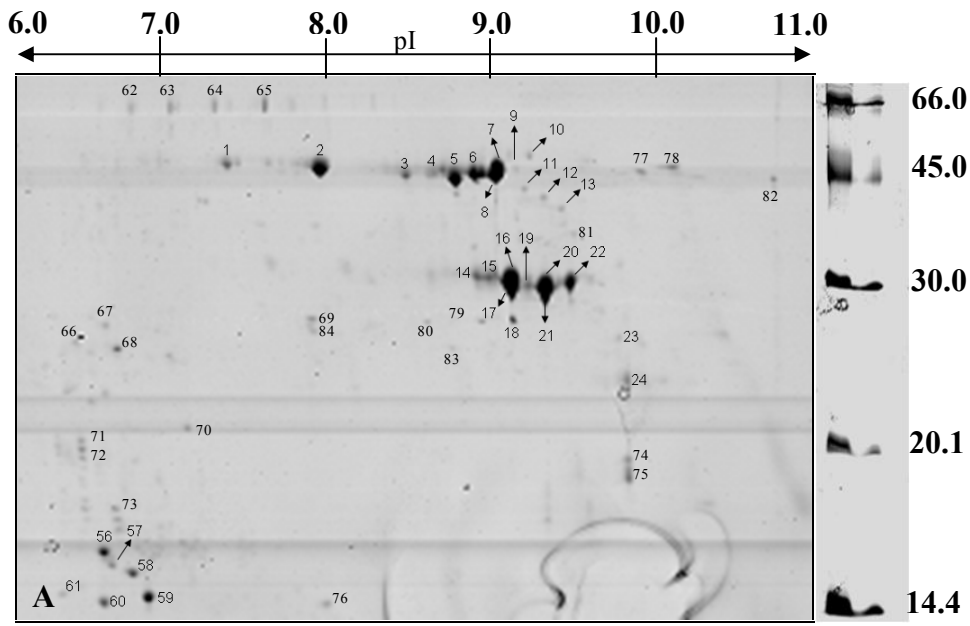




**Figure 3**

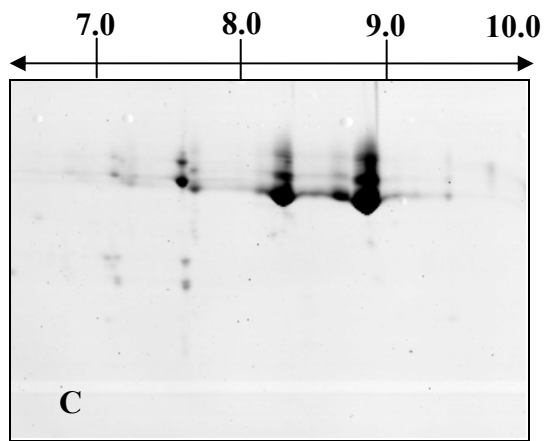
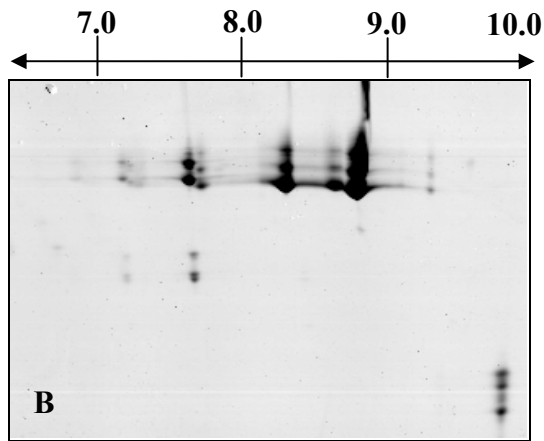
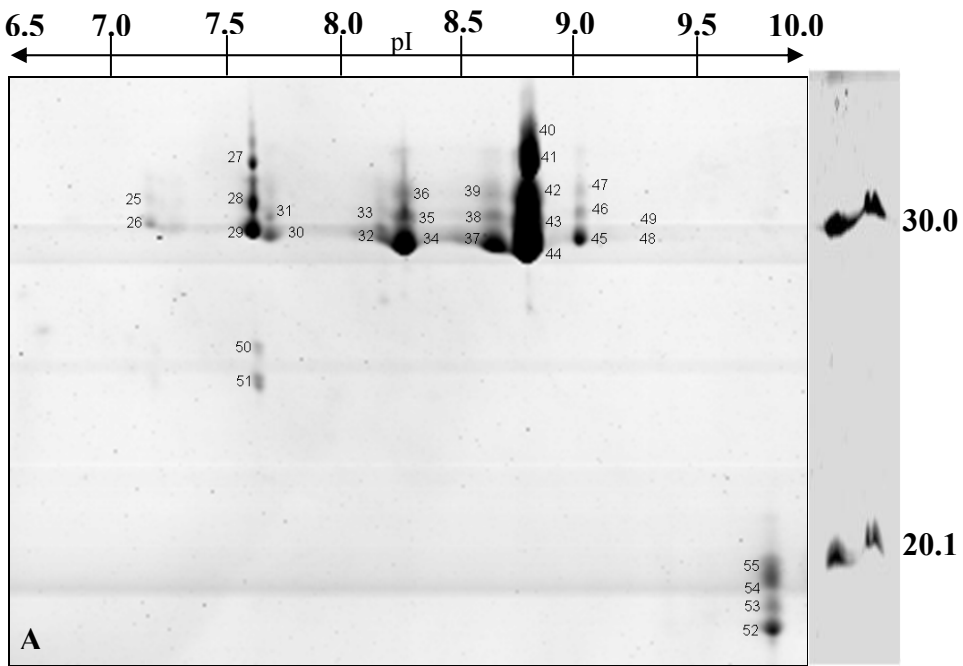


**Figure 4.**

```
TAXI-IIb      EGPLVLAPVTKDTATS LY T IPFH D GANLVLDVAGPLVWSTCDGGQPPAEIPCSSPTCLLA 60
TAXI-IV      KGLPVLAPVTKDTATS LY T IPFH D GANLVLDVAGPLVWSTCDGGQPPAEIPCSSPTCLLA 59
TAXI-Ib/III  KGLPVLAPVTKDTATS LY T IPFH D GASLVLDVAGPLVWSTCEGSQPPAEIPCSSPTCLLS 60
TAXI-IIa     KGLPVLAPVTKDTATS LY T IPFH D GASLVLDVAGLLVWSTCEGGQSPA EIACSSPTCLLA 60
TAXI-725ACCN --LPV L APVTKDPATSLYTIPFH D GASLVLDVAGPLVWSTCEGGQPPAEIPCSSPTCLLA 58
TAXI-725ACC  KGLPVLAPVTKDTATS LY T IPFH D GASLVLDVAGPLVWSTCDGGQPPAEIPCSSPTCLLA 60
TAXI-Ia     --LPV L APVTKDPATSLYTIPFH D GASLVLDVAGPLVWSTCDGGQPPAEIPCSSPTCLLA 58
             ***** . ***** . ***** ***** : * . * . ***** . ***** :
TAXI-IIb     NAYPAPGCPAPSCGSDR HDK PCTAY PYNPVTGACAAGSLFHTK FVAN TTDGNKPVSKVNV 120
TAXI-IV      NAYPAPGCPAPSCGSDR HDK PCTAY PYNPVTGACAAGSLFHTK FVAN TTDGNKPVSKVNV 118
TAXI-Ib/III  NAYPAPGCPAPSCGSDR HDK PCTAY P SNPVTGACAAGSLFHTK FAAN TTDGNKPVSEVNV 120
TAXI-IIa     NAYPAPGCPAPSCGSDR HDK PCTAY P SNPVTGACAAGSLFHTRFAAN TTDGNKPVSEVNV 120
TAXI-725ACCN NAYPAPGCPAPSCGSDTHDKPCTAY PYNPVTGACAAGSLFHTRFAAN TTDGSKPVSKVNV 118
TAXI-725ACC  NAYPAPGCPAPSCGSDKHDKPCTAY PYNPVTGACAAGSLFHTRFAAN TTDGSKPVSKVNV 120
TAXI-Ia     NAYPAPGCPAPSCGSDKHDKPCTAY PYNPVS GACAAGSLSHTRFVAN TTDGSKPVSKVNV 118
             ***** * ***** * * * * : ***** * * : * . ***** . ***** : * *
TAXI-IIb     GVVAACAPSKLLASLPRGSTGVAGLADSG LALPAQVASAQKVANRFL LCLPTGGLGVAIF 180
TAXI-IV      GVVAACAPSKLLASLPRGSTGVAGLADSG LALPAQVASAQKVANRFL LCLPTGGLGVAIF 178
TAXI-Ib/III  GVLAACAPSKLLASLPRGSTGVAGLANSG LALPAQVASTQKVANRFL LCLPTGGLGVAIF 180
TAXI-IIa     RVLAACAPSKLLASLPRGSTGVAGLAGSGLALPSQVASAQKVANKFL LCLPTGGPGVAIF 180
TAXI-725ACCN GVLAACAPSKLLASLPRGSTGVAGLADSG LALPAQVASAQKVAKRFL LCLPTGGPGVAIF 178
TAXI-725ACC  GVLAACPPSKLLASLPRGSTGVAGLADSG LALPAQVASAQKVANRFL LCLPTGGPGVAIF 180
TAXI-Ia     GVLAACAPSKLLASLPRGSTGVAGLANSG LALPAQVASAQKVANRFL LCLPTGGPGVAIF 178
             * : * * . ***** . ***** . ***** : * * : * * : * * : * * : * * * * *
TAXI-IIb     GGGPLPWPQFTQSM DY TPLVAKGGSPAHIYISLKSIKVENTRVPVSERALATGGVMLSTR L 240
TAXI-IV      GGGPLPWPQFTQSM DY TPLVAKGGSPAHIYISLKSIKVENTRVPVSERALATGGVMLSTR L 237
TAXI-Ib/III  GGGPLPWPQFTQSM DY TPLVAKGGSPAHIYISLKSIKVENTRVPVSERALATGGVMLSTR L 240
TAXI-IIa     GGGPLPWPQFTQSM DY TPLVAKGGSPAHIYSARSIKVENTRVPISERALATGGVMLSTR L 240
TAXI-725ACCN GGGPLPWPQFTQSM PY TPLVTKGGSPAHIYSARFIEVGDTRVPVSE GALATGGVMLSTR L 238
TAXI-725ACC  GGGPVWPQFTQSM PY TPLVTKGGSPAHIYSARFIEVGDTRVPVSE GALATGGVMLSTR L 240
TAXI-Ia     GGGPVWPQFTQSM PY TPLVTKGGSPAHIYSARSIVGDTRVPVSE GALATGGVMLSTR L 238
             ***** : ***** * * * * : * * : * * : * * : * * : * * : * *
TAXI-IIb     PYVLLRRDVYRPFVDAFTKALAAQPAN ^ GAPVARAVKPVAPFELCYDTKSLGNNLGGYWVP 300
TAXI-IV      PYVLLRRDVYRPFVDAFTKALAAQPAN ^ GAPVARAVKPVAPFELCYDTKSLGNNLGGYWVP 297
TAXI-Ib/III  PYVLLRRDVYRPFVGAFTKALAAQPAN ^ GAPVARAVKPVAPFELCYDTKSLGNNLGGYWVP 300
TAXI-IIa     PYVLLRRDVYRPLVDAFTKALAAQPAN ^ GAPVARAVKPVAPFELCYDTKTLGNNPGGYWVP 300
TAXI-725ACCN PYAVLRRDVYRPLVDAFTKALAAQHAN ^ GAPVARAVEPVAPFGVCYDTKTLGNNLGGYSVP 298
TAXI-725ACC  PYAVLRRDVYRPLVDAFTKALAAQHAN ^ GAPVARAAEPVAPFGVCYDTKTLGNNLGGYSVP 300
TAXI-Ia     PYVLLRPDVYRPLMDAFTKALAAQHAN ^ GAPVARAVEAVAPFGVCYDTKTLGNNLGGYAVP 298
             * * . : * * ***** : . ***** ***** . : * * * * : * * * * * * * * * *
```

TAXI-IIb NVGLAVDGGSD-WAMTGKNSMVDVKPGTACVAFVEMKGVEAGDGRAPAVILGGAQMEDFV 359  
TAXI-IV NVGLAVDGGSD-WAMTGKNSMVDVKPGTACVAFVEMKGVEAGDGRAPAVILGGAQMEDFV 356  
TAXI-Ib/III NVGLAVDGGSD-WAMTGKNSMVDVKPGTACVAFVEMKGVEAGDGRAPAVILGGAQMEDFV 359  
TAXI-IIa NVLELDGGSD-WALTGKNSMVDVKPGTACVAFVEMKGV DAGDSAPAVILGGAQMEDFV 359  
TAXI-725ACCN NVQLALDGGSDTWTMTGKNSMVDVKPGTACVAFVEMKGVEAGDGRAPAVILGGAQMEDFV 358  
TAXI-725ACC NVQLGLDGGSDTWTMTGKNSMVDVKPGTACVAFVEMKGVEAGDGRAPAVILGGAQMEDFV 360  
TAXI-Ia NVQLGLDGGSD-WTMTGKNSMVDVKQGTACVAFVEMKGVAAGDGRAPAVILGGAQMEDFV 357

\*\*\*:\*\*\*\*\*

TAXI-IIb LDFDMEKKRLGFSRLPQFTGCSSFN FARST 389  
TAXI-IV LDFDMEKKRLGFSRLPQFTGCSSFN FAGST 386  
TAXI-Ib/III LDFDMEKKRLGFLRRLPHFTGCGS----- 382  
TAXI-IIa LDFDMEKKRLGFLRRLPHFTGCSSFN FARST 389  
TAXI-725ACCN LDFDMEKKRLGFSRLPHFTGCGGL----- 382  
TAXI-725ACC LDFDMEKKRLGFSRLPHFTGCGGL----- 384  
TAXI-Ia LDFDMEKKRLGFSRLPHFTGCGGL----- 381

\*\*\*\*\* \*\*:

**Figure 5.**

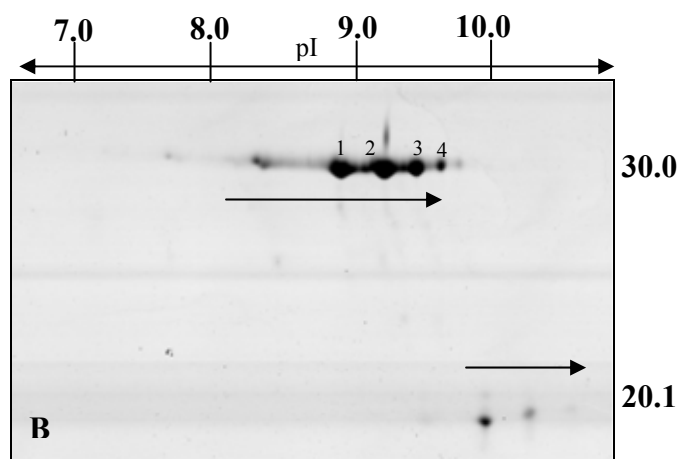
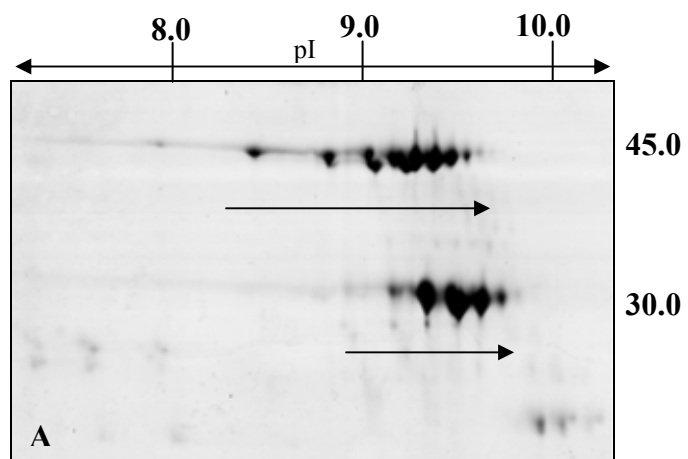


**Figure 6.**

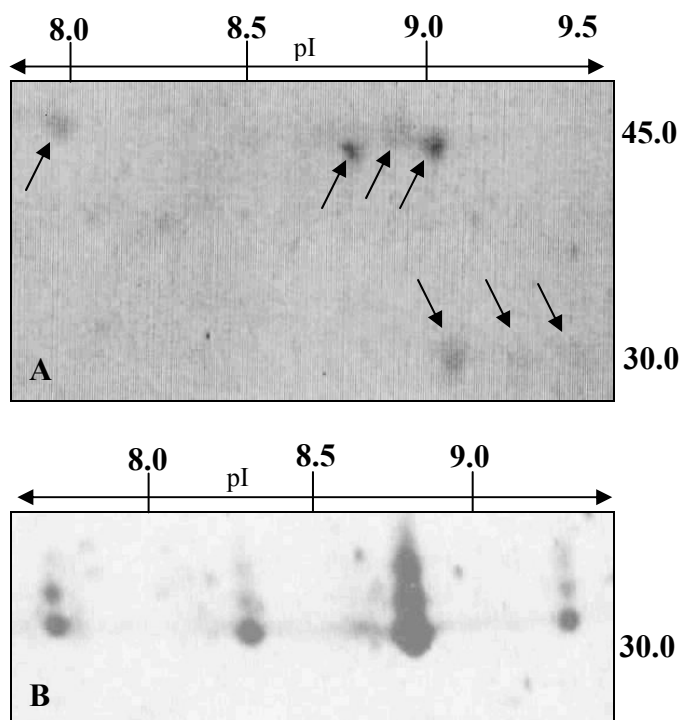


**Figure 7.**

